Available online at www.sciencedirect.com
ScienceDirect
Polymer 47 (2006) 6986–6992
polymer
www.elsevier.com/locate/polymer

Synthesis and optical properties of three novel functional polyurethanes bearing nonlinear optical chromophoric pendants with different π electron conjugation bridge structure

Hongyao Xu [a,d,*], Shouchun Yin [a], Weiju Zhu [a], Yinglin Song [b], Benzhong Tang [c]

[a] Department of Chemistry, Faculty of Chemistry and Chemical Engineering and the Key Laboratory of Environment-Friendly Polymer Materials of Anhui Province, Anhui University, Hefei, Anhui 230039, PR China
[b] Department of Physics, Suzhou University, Suzhou 215008, PR China
[c] Department of Chemistry, Hong Kong University of Science and Technology, Clear Water Bay, Kowloon, Hong Kong, PR China
[d] The State Key Laboratory for Modification of Chemical Fibers and Polymeric Materials & The College of Material Science and Engineering, Dong Hua University, Shanghai 200051, PR China

Received 15 February 2006; received in revised form 17 July 2006; accepted 5 August 2006
Available online 28 August 2006

Abstract

High molecular weight functional polyurethanes bearing large π electron conjugated chromophoric pendants with different conjugation bridge structure, poly(**1a**), poly(**1b**), and poly(**1c**), were synthesized and characterized by FTIR, ^{1}H NMR and UV–vis absorption spectra. Their optical properties were evaluated by optical limiting and nonlinear optical analyses. The results show that these polymers possess good optical limiting and large nonlinear optical properties, which are attributed to the long D–π–A conjugated π electron structure of the NLO-chromophoric segment. Poly(**1a**) with C=C double bond as π electron conjugation bridge shows better optical limiting property than poly(**1b**) and poly(**1c**) with C=N or N=N double bond as conjugation bridge structure under the same linear transmittance, while poly(**1c**) with N=N double bond as π electron conjugation bridge of the NLO-chromophoric segment is superior on nonlinear optical properties to poly(**1a**) and poly(**1b**) with C=C and C=N double bonds as π electron conjugation bridge structure, respectively.

Keywords: Optical limiting; The third-order nonlinear optics; Polyurethane

1. Introduction

The optical materials for the application of limiters in recent years have received significant attention owing to the growing needs for protection of optically sensitive devices and human eyes from laser damage in both civilian and military applications due to the fast development of modern laser technology [1,2]. Among the organic materials, the NLO polymers are considered to be promising materials, mainly because they offer many advantages such as fast time response, light weight, chemical resistance and good processability to form optical devices [3–7].

To enhance the application viability of the organic NLO polymer materials as optical limiter, it is necessary to understand the relationship between the optical limiting property and the molecular structure of the NLO chromophores. The NLO chromophores usually comprise strong electron donor and acceptor groups connected by a π electron conjugation bridge. The increase of the conjugation length and the donor–acceptor strength can improve the optical limiting properties of organic NLO chromophores [8–14], and the large atomic number and the small atomic size may also

* Corresponding author. Department of Chemistry, Faculty of Chemistry and Chemical Engineering and the Key Laboratory of Environment-Friendly Polymer Materials of Anhui Province, Anhui University, Hefei, Anhui 230039, PR China. Tel.: +86 551 5107342; fax: +86 551 5108203.
E-mail address: hongyaoxu@163.com (H. Xu).

0032-3861/$ - see front matter © 2006 Elsevier Ltd. All rights reserved.
doi:10.1016/j.polymer.2006.08.006

enhance the optical limiting properties of the phthalocyanines and porphyrins NLO chromophores [15–18]. However, little attention has been paid to the effect of the different π electron conjugation bridge structure on the optical limiting properties of the NLO chromophores. The different π electronic bridge would be expected to have a significant effect on the ground and excited-state dipole moments and electron transition energies of the molecules and, consequently, could affect the optical limiting property of the NLO chromophores.

In this paper, we synthesized three novel polyurethanes containing nonlinear optical (NLO) chromophores with different π electron conjugation bridge structure, poly(**1a**), poly(**1b**), and poly(**1c**) (Scheme 1), measured their optical limiting and nonlinear optical properties, and investigated the effect of π electron conjugation bridge structure on the optical limiting and nonlinear optical properties of polyurethanes.

2. Experimental

2.1. Materials

4-Bromo-4′-(*N*,*N*-dihydroxyethylamino)stilbene, 4-bromo-4′-(*N*,*N*-dihydroxyethylamino)azobenzene and *N*-((4-*N*,*N*-dihydroxyethylamino)benzylidene)-4-bromoaniline were synthesized according to the method reported [3,4]. 4-Vinylpyridine was purchased from Fluka and distilled over calcium hydride under reduced pressure before use. Palladium(II) acetate was purchased from Aldrich, kept under an inert atmosphere in a glove box, and used as received without further purification. 4,4′-Methylenebis(phenyl isocyanate) (MDI) was purchased from Bayer and purified by distillation under reduced pressure before use. Dibutyltin dilaurate and 1,4-butanediol were purchased from Shanghai Chemical Reagent Company and distilled before use. *N*,*N*-Dimethylformamide (DMF) was purified by distillation over CaH_2 prior to utilization.

2.2. Instruments

FTIR spectra were recorded as KBr pellets on a Nicolet 170SX spectrometer. ^{1}H NMR spectra were obtained on an AVANCE/DMX-300 MHz Bruker NMR spectrometer. Elementary analyses were conducted on Elementary Vario EL-III elementary analysis apparatus. Melting points (mp) were measured on a Yanaco micromelting point apparatus. UV–vis spectra were recorded on a Shimadzu UV-265 spectrometer

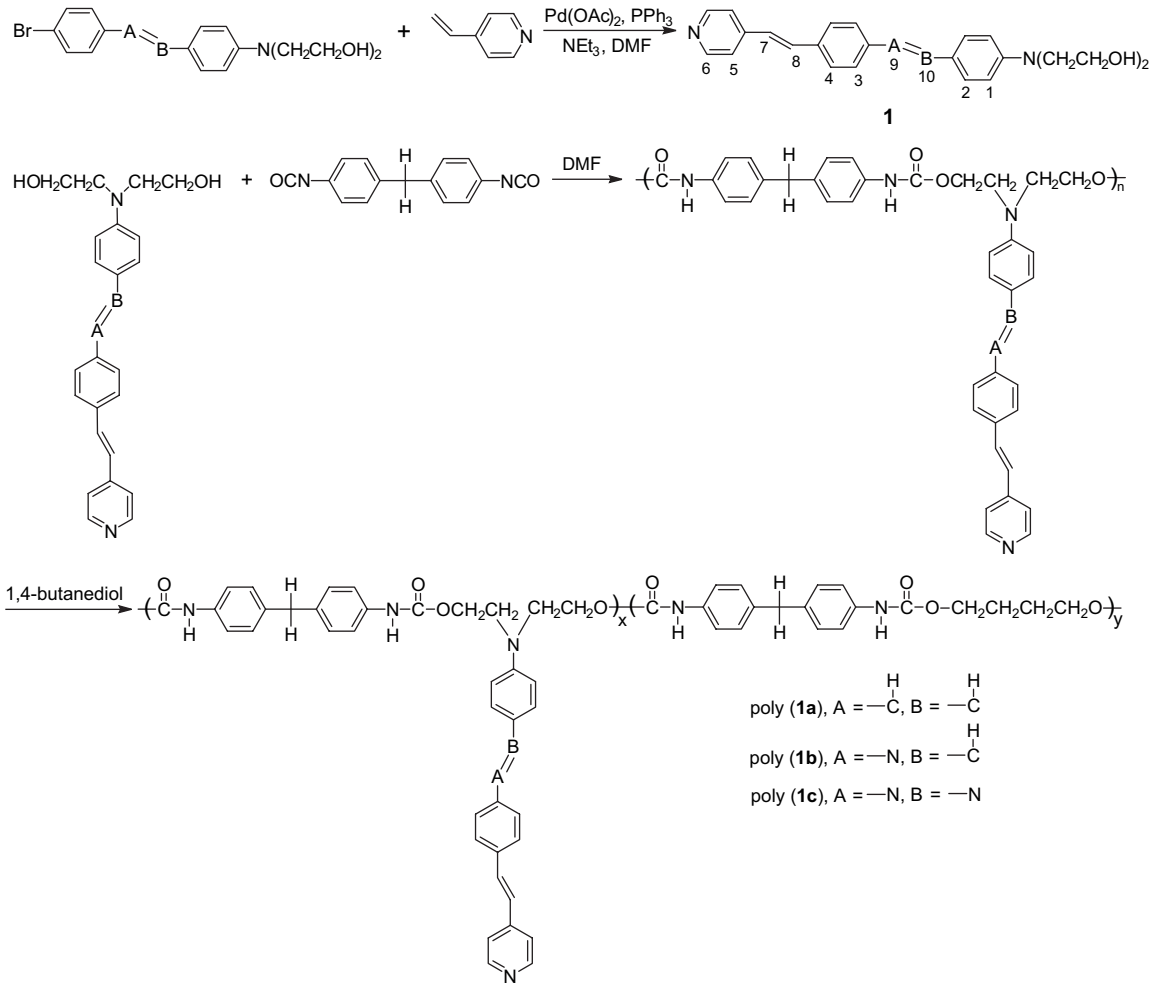

Scheme 1. Synthetic scheme of the functional polyurethane.

using a 1-cm square quartz cell. Molecular weights of the polymers were estimated on KNAVER Vapour Pressure Osmometer.

The optical limiting properties were measured in DMF solutions. Testing was performed using a frequency-doubled, Q-switched, mode-locked continuum ns/ps Nd:YAG laser, which provides linearly polarized 8 ns optical pulses at 532 nm wavelength with a repetition of 1 Hz. The experimental arrangement is similar to that in the literature [3,4]. The transverse mode of the laser pulses is nearly Gaussian. The input laser pulses were split into two beams by an attenuator (Newport). One was employed as reference to monitor the incident laser energy, and the other was focused onto the sample cell by using a lens with 30 cm focal length. The sample was positioned at the focus and housed in quartz cells with a thickness of 5 mm. The incident and transmitted laser pulses were monitored by utilizing two energy detectors, D_1 and D_2 (Rjp-735 energy probes, Laser Precision).

The nonlinear optical properties of the polymers were evaluated by a *Z*-scan technique using the same laser system as in the optical limiting experiment. The experimental set up can be found in the literature [19]. The input energy was 100 μJ. The sample solution was placed in a 2 mm quartz cell and moved along the axis of the incident beam (*z* direction).

2.3. Synthesis

2.3.1. 4′-(*N*,*N*-Dihydroxyethylamino)-4-(pyridine-4-vinyl)-stilbene (**1a**)

Under nitrogen, 1.81 g (5 mmol) 4-bromo-4′-(*N*,*N*-dihydroxyethylamino)stilbene, 11.2 mg (0.05 mmol) $Pd(OAc)_2$, 26.2 mg (0.10 mmol) PPh_3, 0.07 mL (7.5 mmol) 4-vinylpyridine were dissolved in 50 mL DMF. The resultant mixture was refluxed for 24 h. After cooling to room temperature, the reaction solution was put into water to precipitate the product. The precipitate was recrystallized from ethanol for three times to give yellow-green powder in 80% yield. T_m (melting temperature) = 283–285 °C. ^{1}H NMR (DMSO-d_6): $\delta = 3.52$ (4H, t, $J = 6.0$ Hz, CH_2CH_2OH), 3.55 (4H, t, CH_2CH_2OH), 4.70 (2H, s, O*H*), 6.70 (2H, d, $J = 8.6$ Hz, H^1), 7.02 (1H, d, $J = 16.3$ Hz, H^7), 7.18 (1H, d, $J = 16.4$ Hz, H^{10}), 7.21 (1H, d, H^9), 7.40 (2H, d, $J = 8.5$ Hz, H^4), 7.41 (1H, s, H^8), 7.55 (2H, d, H^3), 7.57 (2H, d, H^2), 7.62 (2H, d, $J = 8.1$ Hz, H^5), 8.53 (2H, d, H^6) (for serial number of hydrogen atom see Scheme 1). FTIR (KBr), ν (cm^{-1}): 3374 (O–H), 1588, 1520, 827 (Ar). Elem. Anal. Calcd for $C_{25}H_{26}N_2O_2$: C, 77.72; H, 6.74; N, 7.25. Found: C, 77.65; H, 6.73; N, 7.21.

2.3.2. *N*-((4-*N*,*N*-Dihydroxyethylamino)benzylidene)-4-(pyridine-4-vinyl)aniline (**1b**)

This was prepared as above from *N*-((4-*N*,*N*-dihydroxyethylamino)benzylidene)-4-bromoaniline. The precipitate was recrystallized from ethanol for three times to give brown-yellow solid powder in 81% yield. $T_m = 289$–291 °C. ^{1}H NMR (DMSO-d_6): $\delta = 3.52$ (4H, t, $J = 6.0$ Hz, CH_2CH_2OH), 3.59 (4H, t, CH_2CH_2OH), 4.78 (2H, s, O*H*), 6.82 (2H, d, $J = 8.7$ Hz, H^1), 7.20 (1H, d, $J = 16.3$ Hz, H^7), 7.25 (2H, d, $J = 8.3$ Hz, H^4), 7.54 (1H, d, H^8), 7.56 (2H, d, H^3), 7.68 (2H, d, H^2), 7.73 (2H, d, $J = 8.5$ Hz, H^5), 8.47 (1H, s, C*H*=N), 8.55 (2H, d, H^6). FTIR (KBr), ν (cm^{-1}): 3413 (O–H), 1604, 1576, 825 (Ar). Elem. Anal. Calcd for $C_{24}H_{25}N_3O_2$: C, 74.42; H, 6.46; N, 10.85. Found: C, 74.41; H, 6.59; N, 10.88.

2.3.3. 4′-(*N*,*N*-Dihydroxyethylamino)-4-(pyridine-4-vinyl)-azobenzene (**1c**)

This was prepared as above from 4-bromo-4′-(*N*,*N*-dihydroxyethylamino)azobenzene. The precipitate was recrystallized from ethanol for three times to give red-brown powder in 80% yield. $T_m = 297$–299 °C. ^{1}H NMR (DMSO-d_6): $\delta = 3.56$ (4H, t, $J = 6.0$ Hz, CH_2CH_2OH), 3.60 (4H, t, CH_2CH_2OH), 4.88 (2H, s, O*H*), 6.86 (2H, d, $J = 8.9$ Hz, H^1), 7.37 (1H, d, $J = 16.3$ Hz, H^7), 7.64 (2H, d, $J = 7.7$ Hz, H^4), 7.72 (1H, d, H^8), 7.77 (2H, d, H^3), 7.80 (2H, s, H^2), 7.82 (2H, d, $J = 8.1$ Hz, H^5), 8.58 (2H, d, H^6). FTIR (KBr), ν (cm^{-1}): 3373 (O–H), 1598, 1512, 823 (Ar). Elem. Anal. Calcd for $C_{23}H_{24}N_4O_2$: C, 71.13; H, 6.19; N, 14.43. Found: C, 71.44; H, 6.25; N, 14.45.

2.4. Polymerization

All the polymerization reactions and manipulations were performed under nitrogen, except for the purification of the polymers, which was conducted in an open atmosphere. A typical procedure is given below: to a 50 mL four-necked cylindrical vessel equipped with a mechanical stirrer, 5 mmol diol **1**, 2.62 g (11 mmol) MDI and 0.1 mL dibutyltinlaurate in 25 mL *N*,*N*-dimethylacetamide were added with stirring of the solution under nitrogen. Then the mixture was reacted at 80 °C for 3 h to make prepolymerization. 1,4-Butanediol (0.45 g (5 mmol)) was added dropwise to the reaction mixture and the remaining isocyanate group was intermittently checked by di-*n*-butylamine back-titration during polymerization to determine the progress of polymerization. The reaction mixture became very sticky with polymerization, and it was carried out until the unreacted isocyanate group was completely used. The polymer solution was poured dropwise into 250 mL of methanol. The precipitated polyurethane was collected by filtration and redissolved in DMF and precipitated into methanol for purification. The dissolution–precipitation process was repeated for three times, and the finally isolated precipitant was dried under vacuum at 50 °C to a constant weight.

Poly(**1a**): yellow-green solid; yield: 91.5%; M_n (number average molecular weight) = 10 800 (VPO). ^{1}H NMR (DMSO-d_6): $\delta = 2.55$–3.12 ($-CH_2C_2H_4CH_2-$), 3.22–4.38 ($N(CH_2CH_2O)_2$, $N(CH_2CH_2O)_2$, $-CH_2C_2H_4CH_2-$ and $-ArCH_2Ar-$), 6.51–8.75 (Ar–*H* and $-CH=CH-$), 9.63 (N*H*CO–). FTIR (KBr), ν (cm^{-1}): 3305 (N–H), 1652 (C=O), 1595, 1509, 828 (Ar).

Poly(**1b**): orange-red solid; yield: 92.1%; $M_n = 10\,500$ (VPO). ^{1}H NMR (DMSO-d_6): $\delta = 2.68$–3.05 ($-CH_2C_2H_4CH_2-$), 3.31–4.29 ($N(CH_2CH_2O)_2$, $N(CH_2CH_2O)_2$, $-CH_2C_2H_4CH_2-$ and $-ArCH_2Ar-$), 6.73–8.62 (Ar–*H*, $-CH=N-$ and

–C*H*=C*H*–), 9.55 (N*H*CO–). FTIR (KBr), ν (cm^{-1}): 3302 (N–H), 1658 (C=O), 1593, 1510, 825 (Ar).

Poly(**1c**): deep-red solid; yield: 92.7%; $M_n = 11\,700$ (VPO). ^{1}H NMR (DMSO-d_6): $\delta = 2.69$–2.93 ($-CH_2C_2H_4CH_2-$), 3.05–4.35 ($N(CH_2CH_2O)_2$, $N(CH_2CH_2O)_2$, $-CH_2C_2H_4CH_2-$ and $-ArCH_2Ar-$), 6.75–8.63 (Ar–H and –C*H*=C*H*–), 9.60 (N*H*CO–). FTIR (KBr), ν (cm^{-1}): 3303 (N–H), 1648 (C=O), 1596, 1512, 824 (Ar).

3. Results and discussion

3.1. Polymer structure

Fig. 1 shows the FTIR spectra of **1c**, poly(**1a**), poly(**1b**) and poly(**1c**). The characteristic O–H stretching vibration at 3373 cm^{-1} of the monomer **1c** disappears and the characteristic stretching vibrations ν_s (N–H) and ν_s (C=O) at 3306 and 1648 cm^{-1}, respectively, are also found in the spectrum of its polymer, conforming the formation of the urethane group.

Fig. 2 shows the ^{1}H NMR spectra of monomer **1a** and poly(**1a**) in DMSO-d_6. The hydroxyl proton of **1a** absorbs at $\delta = 4.72$ ppm, which disappears in the spectrum of its polymer. A new broad resonance peak, assigned to the urethane proton absorption at $\delta = 9.63$ ppm, is emerged on the spectrum of poly(**1a**) [20,21], further displaying the formation of urethane linkage. All other resonance peaks of the segments of **1a**, 1,4-butanediol and 4,4′-methylenebis(phenyl isocyanate) appear in the spectrum of poly(**1a**). The relative ratios of integration of these protons are also consistent with the proposed structures, as shown in Scheme 1, further conforming that functional polyurethane polymers are prepared.

The ^{1}H NMR spectrum was also used to determine the chromophoric content in the polymer. Provided that x represents the peak area of one proton of the **1a** segment and y is the peak area of one proton of the 1,4-butanediol segment. The content of the **1a** segment may be estimated by directly comparing the peak area of all methylene protons with the peak area of all aryl protons based on the following equation:

$$[16x + 8(x+y)] : [8y + 2(x+y) + 8x] = A_{Ar} : A_{me} \quad (1)$$

where A_{Ar} corresponds to the absorption peak area of all aryl protons of the **1a** and MDI segments. A_{me} is associated with the peak areas of all methylene protons of the **1a**, MDI and 1,4-butanediol segments. $16x$ is corresponding to the peak areas of 16 aryl protons of the **1a** segment and $8(x+y)$ is corresponding to the peak areas of eight aryl protons of the MDI segment. Thus, the **1a** component content in the polyurethane was calculated according to Eq. (1):

$$\text{The } \mathbf{1a} \text{ segment content (mol\%)} = \frac{x}{x+y} \times 100\%$$

$$= \frac{A_{Ar} - 0.8A_{me}}{1.6A_{me}} \times 100\% = 24.5\%$$

The **1b** and **1c** component contents in the polyurethane were calculated to be 24.9% and 23.8%, respectively, indicating that the content of chromophores in the polymers is little affected by the π electron conjugation bridge structure of the NLO chromophores.

The UV–vis spectra of the objective polymers poly(**1a**), poly(**1b**) and poly(**1c**) in DMF are shown in Fig. 3. Poly(**1a**) exhibits the absorption peak at 408 nm associated with the π–π* transition of the extended π electron conjugation of the NLO-chromophoric segment. The maximum UV–vis spectra absorption of poly(**1b**) shifts from 408 nm of poly(**1a**) to 386 nm when one carbon of C=C is replaced by nitrogen. On the contrary, the maximum UV–vis spectra absorption of poly(**1c**) shifts from 408 nm of poly(**1a**) to 463 nm when both carbons of C=C are replaced by nitrogen, hinting that the π electron conjugation bridge structure has significant

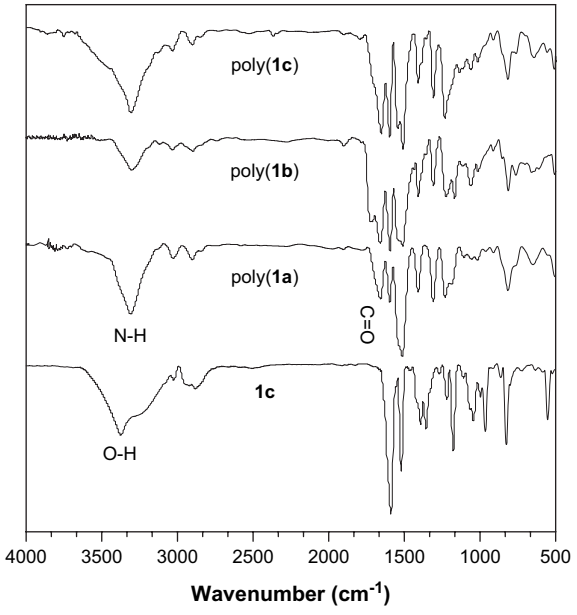

Fig. 1. FTIR spectra of **1c**, poly(**1a**), poly(**1b**) and poly(**1c**).

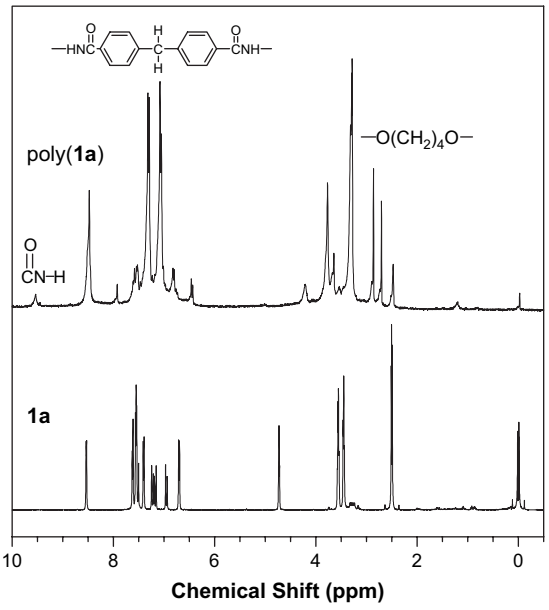

Fig. 2. ^{1}H NMR spectra of **1a** and poly(**1a**) in DMSO-d_6.

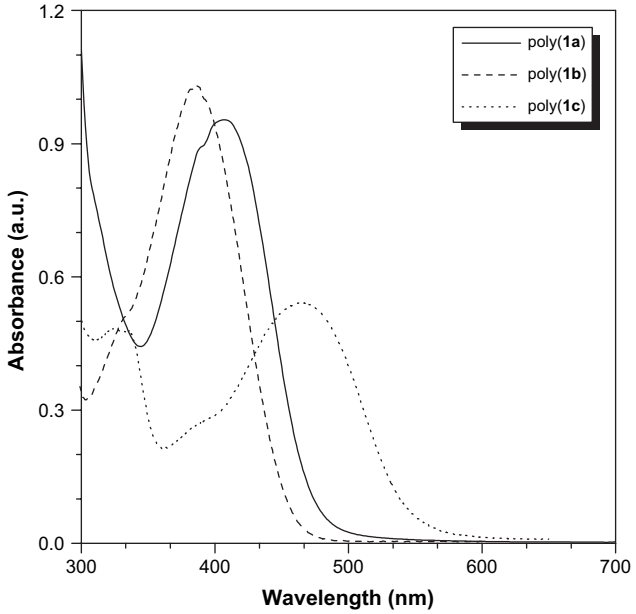

Fig. 3. UV–vis spectra of DMF solutions of poly(**1a**), poly(**1b**) and poly(**1c**) at 20 °C/min.

effect on their ground state electron absorption spectra of molecules.

3.2. Nonlinear optical properties

The nonlinear absorption coefficients of poly(**1a**), poly(**1b**) and poly(**1c**) were measured by using *Z*-scan technique. The results of *Z*-scan with and without an aperture showed that poly(**1a**) and poly(**1b**) have only nonlinear refraction (Figs. 4 and 5) while poly(**1c**) has both nonlinear absorption (Fig. 6a) and nonlinear refraction (Fig. 6b).

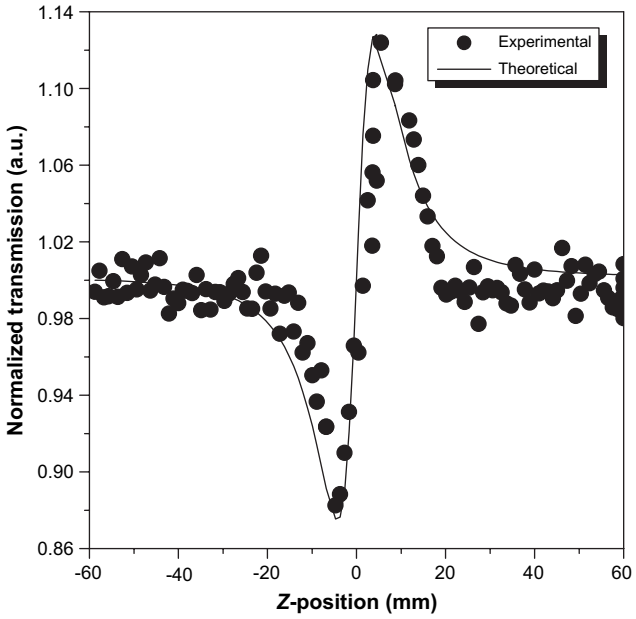

Fig. 4. *Z*-scan data of the DMF solution of poly(**1a**) using an 8 ns, 1 Hz pulses of 532 nm laser light. Solid circle: experimental data; solid line: theoretical curve.

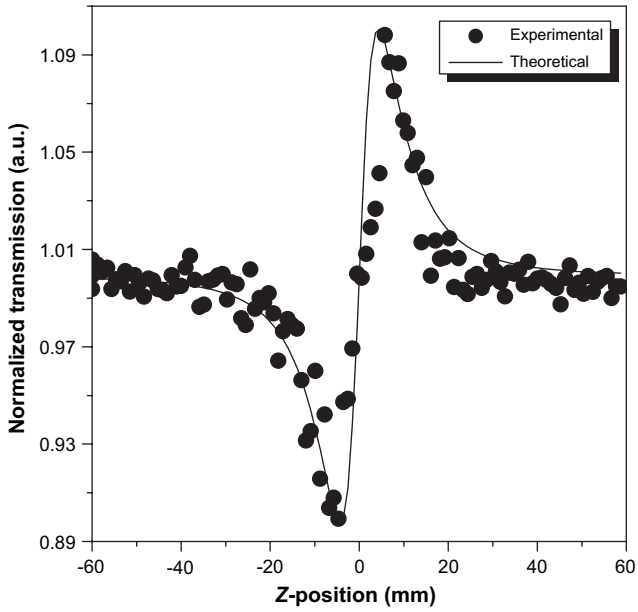

Fig. 5. *Z*-scan data of the DMF solution of poly(**1b**) using an 8 ns, 1 Hz pulses of 532 nm laser light. Solid circle: experimental data; solid line: theoretical curve.

In theory, the normalized transmittance for the open aperture can be written as [4,19]:

$$T(z, s=1) = \sum_{m=0}^{\infty} \frac{[-q_0(z)]^m}{(m+1)^{3/2}}, \qquad \text{for } |q_0| < 1 \tag{2}$$

where $q_0(z) = \alpha_2 I_0(t) L_{\text{eff}}/(1 + z^2/z_0^2)$, α_2 is the nonlinear absorption coefficient, $I_0(t)$ is the intensity of laser beam at focus ($z = 0$), $L_{\text{eff}} = [1 - \exp(-\alpha_0 L)]/\alpha_0$ is the effective thickness with α_0 the linear absorption coefficient and L the sample

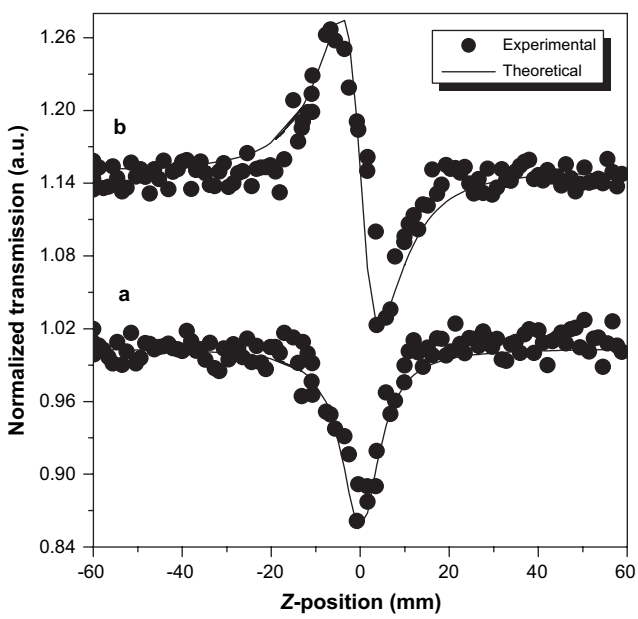

Fig. 6. *Z*-scan data of the DMF solution of poly(**1c**) using an 8 ns, 1 Hz pulses of 532 nm laser light. Solid circle: experimental data; solid line: theoretical curve.

thickness, z_0 is the diffraction length of the beam, and z is the sample position. Thus, the nonlinear absorption coefficients of poly(**1c**) can be determined by fitting the experimental data using Eq. (2).

The normalized transmission for the closed aperture Z-scan is given by the following [4,19]:

$$T(z, \Delta\phi) = 1 + \frac{4\Delta\phi x}{(x^2+9)(x^2+1)} \tag{3}$$

where $x = z/z_0$ and $\Delta\phi$ is on-axis phase change caused by the nonlinear refractive index of the sample and $\Delta\phi = 2\pi I_0(1 - e^{-\alpha_0 L})n_2/\lambda\alpha_0$. Thus, the nonlinear refractive coefficients of poly(**1a**), poly(**1b**) and poly(**1c**) can be determined by fitting the experimental data using Eq. (3).

The $\chi^{(3)}$ can be calculated by the following equation [4,19]:

$$|\chi^{(3)}| = \sqrt{\left|\frac{cn_0^2}{80\pi}n_2\right|^2 + \left|\frac{9\times 10^8 \varepsilon_0 n_0^2 c^2}{4\pi\omega}\alpha_2\right|^2} \tag{4}$$

where ε_0 is the permittivity of vacuum, c is the speed of light, n_0 is the refractive index of the medium and $\omega = 2\pi c/\lambda$. Therefore, the results can be calculated and are listed in Table 1. As shown in Table 1, the nonlinear susceptibilities $\chi^{(3)}$ of poly(**1a**), poly(**1b**) and poly(**1c**) are 5.7×10^{-12}, 3.2×10^{-12} and 6.7×10^{-12} esu, respectively, and the nonlinear susceptibilities of poly(**1a**) and poly(**1c**) are larger than that of poly(**1b**), and poly(**1c**) with N=N double bond as conjugated bridge of the NLO-chromophoric segment shows the largest third-order nonlinearity. Comparing the structures of poly(**1a**), poly(**1b**) and poly(**1c**), it can be seen that they are only different from the π electron conjugation bridge structure of the NLO-chromophoric segment. From the crystal structures of stilbene, *N*-benzilidene aniline and azobenzene [22–24], it is well known that stilbene and azobenzene mainly adopt the planar structure in the molecules while *N*-benzilidene aniline is usually considered to possess the non-planar structure in the molecules due to the distortion of the two adjacent benzene rings along with the single bond. Therefore, the non-planarity of the chromophoric segment may decrease the effective π electron conjugation of the chromophoric segment to result in the low nonlinear susceptibility of poly(**1b**). Simultaneously, the third-order nonlinear susceptibilities $\chi^{(3)}$ of monomers are also measured to be 8.8×10^{-12}, 6.7×10^{-12} and 9.1×10^{-12} esu for monomer **1a**, **1b** and **1c**, respectively. The nonlinear optical property decreases when they are incorporated into polymers, which may result from the lower NLO chromophore content in the polymers.

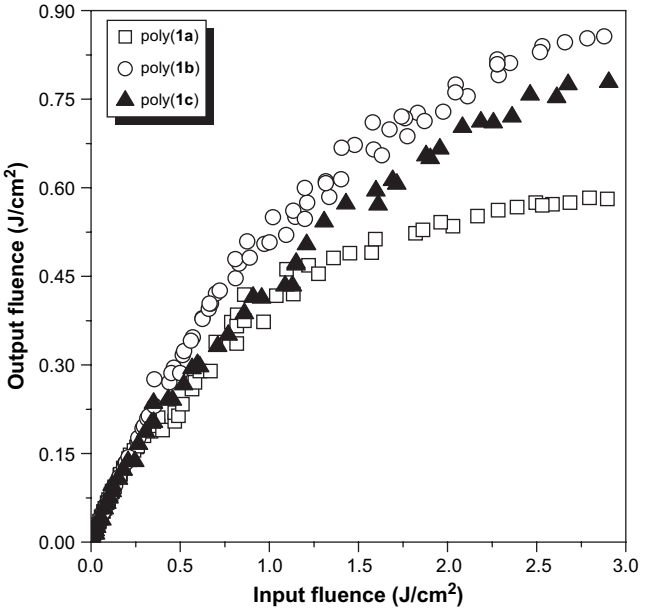

Fig. 7. Optical responses to 8 ns, 1 Hz pulses of 532 nm laser light of poly(**1a**) (open squares), poly(**1b**) (open circles), poly(**1c**) (solid triangles) solutions with a linear transmission of 80%.

3.3. Optical limiting properties

Fig. 7 shows the optical limiting performances of poly(**1a**), poly(**1b**) and poly(**1c**) at the same linear transmittance ($T = 80\%$). As shown in Fig. 7, at very low incident fluence, the output fluence of poly(**1a**), poly(**1b**) and poly(**1c**) solutions with 80% transmittance linearly increases with the incident fluence obeying the Beer–Lambert law. However, at high incident fluence, the transmittance of the solution decreased, and a nonlinear relationship is observed between the output and input fluences, and with a further increase in the incident fluence, the transmitted fluence reaches a plateau (limiting amplitude), showing the good optical limiting property. Simultaneously, the optical limiting properties are significantly affected by the π electron conjugation bridge structure of the chromophoric segment. Poly(**1a**) shows the limiting amplitude at 0.58 J/cm^2 while the limiting amplitudes for poly(**1b**) and poly(**1c**) are at 0.86 J/cm^2 and 0.78 J/cm^2, respectively. Thus, poly(**1a**) shows better optical limiting property than poly(**1b**) and poly(**1c**).

The optical limiting mechanisms of organic compounds are often based on two-photon absorption (TPA) or reverse saturable absorption (RSA). Generally, TPA-based optical limiting effect can be yielded in principle under the laser irradiation of picosecond or shorter pulses. RSA is achieved on a nanosecond or longer time scale, rather than a picosecond time scale,

Table 1
The nonlinear optical properties of poly(**1a**), poly(**1b**) and poly(**1c**)

Polymer	Conc. (mg/mL)	α_2 (m/W)	n_2 (m^2/W)	Im $\chi^{(3)}$ (esu)	Re $\chi^{(3)}$ (esu)	$\chi^{(3)}$ (esu)
Poly(**1a**)	0.117	–	2.33×10^{-18}	–	5.7×10^{-12}	5.7×10^{-12}
Poly(**1b**)	0.133	–	1.52×10^{-18}	–	3.2×10^{-12}	3.2×10^{-12}
Poly(**1c**)	0.083	8.91×10^{-12}	2.25×10^{-18}	3.6×10^{-12}	5.6×10^{-12}	6.7×10^{-12}

owing to the different excited-state lifetimes involved in a multilevel energy process [12]. In this work, the polymers are excited by the laser with 8 ns pulse width at 532 nm wavelength and the transmittance of all these polymers solutions decreases with the increase of the incident fluence. Therefore, we consider that the optical limiting properties of poly(**1a**), poly(**1b**) and poly(**1c**) may mainly arise from RSA.

The optical limiting property of the organic compounds for RSA mechanism depends on the ratio of the excited-state absorption cross-section (σ_{ex}) to the ground state absorption cross-section (σ_0) of molecules, which was defined as $\sigma_{ex}/\sigma_0 = \ln T_{sat}/\ln T_0$. T_{sat} is the saturated transmittance for high degrees of excitation [25]. In our experimental set up, the damage threshold for the sample cell limits the maximum fluence; therefore, we are unable to reach the saturable transmittance for these compounds. Nevertheless, we can use the transmittance at 2.9 J/cm^2 to calculate the lowest bound for σ_{ex}/σ_0. It is seen from Fig. 3 that poly(**1c**) shows strong ground state electron absorption at 532 nm wavelength, hinting that poly(**1c**) has large ground state absorption cross-section, while poly(**1a**) displays weak ground state electron absorption at 532 wavelength, showing that poly(**1a**) may possesses small ground state absorption cross-section to result in larger ratio of σ_{ex}/σ_0 than poly(**1c**). As shown in Fig. 7, the corresponding value of σ_{ex}/σ_0 for poly(**1a**) is calculated to be 7.21, while σ_{ex}/σ_0 for poly(**1c**) is 5.87. It may be why poly(**1a**) shows better optical limiting property than poly(**1c**) although that poly(**1c**) displays better nonlinear optical property than poly(**1a**).

4. Conclusion

We have successfully synthesized three novel functional polyurethanes bearing nonlinear optical chromophores with different π electron conjugation bridge structure in high yield. The incorporation of NLO chromophore into polyurethanes endowed polyurethanes' novel nonlinear optical and optical limiting properties. Simultaneously, it is found that the optical limiting and nonlinear optical performance are strongly affected by π electron conjugation bridge structure of the NLO chromophores. The polymer with N=N double bond as π electron conjugation bridge structure shows the best nonlinear optical property and the polymer with C=C double bond as π electron conjugation bridge structure displays the best optical limiting property, which is attributed to the large σ_{ex}/σ_0. The work provides a novel path for designing new optical materials with good optical limiting property.

Acknowledgements

This research was financially supported by the National Natural Science Fund of China (Grant Nos. 90206014 and 50472038), the Program for New Century Excellent Talents in University (NCET-04-0588), the Excellent Youth Fund of Anhui Province (Grant No. 04044060), and the Award for High Level Intellectuals (Grant No. 2004Z027) from Anhui Province.

References

[1] Tutt LW, Kost A. Nature 1992;356:225.
[2] Tutt LW, Boggess TF. Prog Quantum Electron 1993;17:299.
[3] Yin SC, Xu HY, Shi WF, Gao YC, Song YL, Lam JWY, et al. Polymer 2005;46:7670.
[4] Yin SC, Xu HY, Fang M, Shi WF, Gao YC, Song YL. Macromol Chem Phys 2005;206:1549.
[5] Burland DM, Miller RD, Walsh C. Chem Rev 1994;94:31.
[6] Marks TJ, Ratner MA. Angew Chem Int Ed Engl 1995;34:155.
[7] Dalton LR, Harper AW, Ghosen R, Laquindanum J, Liang Z, Hubble A, et al. Adv Mater 1995;7:519.
[8] Qureshi FM, Martin SJ, Long X, Bradley DDC, Henari FZ, Blau WJ, et al. Chem Phys 1998;231:87.
[9] Yin SC, Xu HY, Su XY, Gao YC, Song YL, Lam JWY, et al. Polymer 2005;46:10592.
[10] Zhou GJ, Zhang S, Wu PJ, Ye C. Chem Phys Lett 2002;363:610.
[11] Sun WF, Wu ZX, Yang QZ, Wu LZ, Tung CH. Appl Phys Lett 2003;82:850.
[12] Sun WF, Bader MM, Carvalho T. Opt Commun 2003;215:185.
[13] Qu SL, Gao YC, Zhao CJ, Wang YX, Fu SY, Song YL, et al. Chem Phys Lett 2003;367:767.
[14] Anderson HL, Martin SJ, Bradeley DC. Angew Chem Int Ed Engl 1994;33:655.
[15] Spanglar CW. J Mater Chem 1999;9:2013.
[16] Liu HW, Chen CF, Xi F, Wang P, Zhang S, Wu PJ, et al. J Nonlinear Opt Phys Chem 2001;4:423.
[17] Kiran PP, Srinivas NKMN, Reddy DR, Maiya BG, Dharmadhikari A, Sandhu AS, et al. Opt Commun 2002;202:347.
[18] Frutos EMG, O'Flaberty SM, Maya EM, Torre GDL, Blau W, Vazquez P, et al. J Mater Chem 2003;13:749.
[19] BaHae MS, Said AA, Wei TH, Hagan DJ, Stryland EWV. IEEE J Quantum Electron 1990;26:760.
[20] Lee JY, Bang HB, Park EJ, Baek CS, Rhee BK, Lee SM. Synth Met 2004;144:159.
[21] Lee JY, Bang HB, Kang TS, Park EJ. Eur Polym J 2004;40:1815.
[22] Nakai H, Ezumi K, Shiro M. Acta Crystallogr Sect B Struct Sci 1981;37:193.
[23] Morley JO. J Mol Struct 1995;340:45.
[24] Morley JO. J Chem Soc Perkin Trans 1995;2:731.
[25] Perry JW, Mansour K, Marder SR, Perry K, Alvarez D, Choog I. Opt Lett 1994;19:625.